ENVIRONMENTAL REPORTS

Review Article
ISSN: 3041-556X
Journal homepage: https://er.researchfloor.org/

A Comparative Study of Chemically Enhanced Crustacean Shell Carbons for Sustainable Adsorbent Development in Polycyclic Aromatic Hydrocarbon (PAH) Sequestration

Akomah, Uchechi[1], Nwaogazie, Ify L*[2]., Akaranta, Onyewuchi[3], Udeh, Ngozi U.[2], Ikebude, Chiedozie F.[2], and Amuchi, Otunyo G.[2]

[1]*World Bank Africa Centre of Excellence in Oilfields Chemicals Research, University of Port Harcourt, Choba, Port Harcourt, Rivers State, Nigeria.*
[2]*Department of Civil and Environmental Engineering, University of Port Harcourt, Choba, Port Harcourt, Rivers State, Nigeria.*
[3]*Department of Industrial Chemistry, University of Port Harcourt, Choba, Port Harcourt, Rivers State, Nigeria.*

Citation: Akomah, Uchechi, Nwaogazie, Ify L., Akaranta, Onyewuchi, Udeh, Ngozi U., Ikebude, Chiedozie F., and Amuchi, Otunyo G. (2025). A Comparative Study of Chemically Enhanced Crustacean Shell Carbons for Sustainable Adsorbent Development in Polycyclic Aromatic Hydrocarbon (PAH) Sequestration. *Environmental Reports; an International Journal*.
DOI: https://doi.org/10.51470/ER.2025.7.1.103

Corresponding Author: **Nwaogazie, Ify L** | E-Mail: **(ifynwaogazie@yahoo.com)**

Received 28 February 2025 | Revised 26 March 2025 | Accepted April 29 2025 | Available Online May 27 2025

ABSTRACT

The study aims to develop enhanced adsorbent Polycyclic Aromatic Hydrocarbon (PAH) Sequestration using crustacean shell carbons. Activated carbon was produced from periwinkle shells, clam shells, whelk shells, and a 1:1 composite of clam and whelk shells through carbonization at 450 °C under limited oxygen, followed by chemical activation with H_2SO_4 at 750 °C and KOH at 650 °C. This process resulted in eight adsorbents: Periwinkle Shell Acid-Activated Carbon (PSAAC), Periwinkle Shell Base- Activated Carbon (PSBAC), Clam Shell Acid-Activated Carbon (CSAAC), Clam Shell Base- Activated Carbon (CSBAC), Whelk Shell Acid-Activated Carbon (WSAAC), Whelk Shell Base- Activated Carbon (WSBAC), Clam-Whelk Shell Acid-Activated Carbon (CWSAAC), and Clam- Whelk Shell Base-Activated Carbon (CWSBAC). Characterization using Fourier Transform Infrared Spectroscopy (FTIR) and physicochemical analysis showed that CSBAC had the highest surface area (1288 m^2/g) and bulk density (0.687 g/cm^3). Batch adsorption experiments were conducted to evaluate the influence of adsorbent dosage and contact time on Polycyclic Aromatic Hydrocarbon (PAH) removal from contaminated water samples. CSBAC exhibited the highest removal efficiency, reaching 98.94% at a 1 g dosage with an adsorption capacity of 2.315 mg/g. Adsorption isotherms were analyzed using Langmuir, Freundlich, Henry, Elovich, and Janovich models. The Freundlich and Langmuir models best described adsorption for PSAAC, PSBAC, CSAAC, CSBAC, CWSAAC, and CWSBAC, with PSBAC achieving the highest Langmuir monolayer adsorption capacity (31.688 mg/g). In contrast, the Henry isotherm best represented PAH adsorption for WSAAC and WSBAC. Comparative analysis of acid and base-activated carbon indicated no statistical difference between acid and base activation on removal efficiency of PAH.

Keywords: *Low-cost adsorbents; crustacean shells; H2SO4 activation; KOH activation; periwinkle shells; clam shells; whelk shells; composite shells; Freundlich isotherm; Langmuir isotherm; henry isotherm; Elovich isotherm; Janovich isotherm.*

1. Introduction

The growing emphasis on sustainability in environmental processes has highlighted adsorption techniques as a key approach for contaminant removal in water treatment. Adsorption is a separation process where molecules from a fluid phase (liquid or gas) adhere to the external and internal surfaces of a solid material known as the adsorbent [1]. This process plays a crucial role in environmental protection, pollutant removal, gas purification, and industrial separation processes, making it an essential tool for sustainable development [2]. Adsorption occurs through a mass transfer mechanism, where substances migrate from the liquid phase and bind to a solid surface via physical or chemical interactions [3]. The choice of a suitable adsorbent depends on its application, with key factors such as cost, kinetics, compatibility, selectivity, capacity, and regenerability influencing its effectiveness [4]. Lignocellulosic biomass has been identified as a promising precursor for carbon adsorbents.[5] noted that global lignocellulosic fiber production is estimated at 10–50 billion tons annually, offering vast potential for alternative environmental remediation methods. Biomass-derived carbon adsorbents from agricultural and household residues have been widely used in pollutant removal due to their large internal surface area, mechanical integrity, and regenerability [6]. For low-cost activated carbon, the preferred precursors should be freely available, inexpensive, and environmentally safe [7].

Crustacean shells have emerged as effective and sustainable adsorbents for pollutant removal due to their natural abundance and cost-effectiveness [8]. The key component responsible for their versatility is chitin, the second most abundant biopolymer after cellulose, with approximately 80% of chitin production derived from crustacean shells [9]. Chitin's nitrogen-rich polysaccharide structure provides chemical resistance and mechanical strength, making it suitable for conversion into activated carbon through pyrolysis [10]. Chitin-derived biochar has shown promising applications in water treatment and gas adsorption, further reinforcing its potential as a sustainable adsorbent [11]. To enhance adsorption efficiency, various activation techniques have been developed to modify surface properties and improve adsorption capacity.

This study explores the use of crustacean shell-derived carbons in sustainable water treatment by employing different activation methods and conducting a comparative analysis of their effectiveness in pollutant removal through adsorption studies.

2. Materials and Methods

Preparation of the adsorbent: Periwinkle shells (*Tympanotamus fuscatus*), West African clam shells (*Galatea paradoxa*), and whelk shells (*Buccinum undatum*) were sourced from a local market in Borokiri, Port Harcourt. The shells were soaked in warm water with detergent for four days to remove dust, residual organic matter, and soluble impurities. They were then thoroughly rinsed with tap water under continuous agitation to dislodge any remaining contaminants.

Afterward, the shells were sun-dried for three days and stored in plastic containers before laboratory processing.

To enhance surface properties, the shells were subjected to carbonization in a muffle furnace at 450°C for three hours. The resulting carbonized materials were pulverized into fine powder, sieved through a 75 µm mesh to eliminate larger particles, and stored in plastic containers. The prepared samples were then divided into two equal portions for chemical activation using acidic and basic treatments.*Chemical activation*

Acid Activation: The powdered samples were individually mixed with 0.5 M H_2SO_4 to form a paste, then heated in a muffle furnace at 750°C for two hours. The activated samples were allowed to cool, thoroughly washed with deionized water until the pH reached approximately 6, and then dried in an oven at 105°C for six hours before being stored in airtight containers.

Base Activation: The second portion of the samples was soaked in 0.5 M KOH and mixed to form a paste, followed by heating in a muffle furnace at 650°C for two hours. After cooling, the samples were washed with deionized water, dried in an oven at 105°C for six hours, and stored in airtight containers.

Characterization of Adsorbents: Attenuated Total Reflectance Fourier Transform Infrared Spectroscopy (ATR-FTIR) was performed using AGILENT TECHNOLOGIES CARY 630 FTIR CARY630 ZnSe. PART NO: - G8043 64002, MODEL NO: - MY19322004.A baseline correction

is first performed by measuring the spectrum of the Attenuated Total Reflectance (ATR) crystal without a sample to eliminate background interference. The activated carbon samples are then placed on the ATR crystal, aligned with the infrared beam, and pressed for optimal contact before spectra are recorded by measuring the reflected infrared light. The collected spectra are processed to remove noise and baseline drift, allowing for qualitative and quantitative analysis of the sample's composition and structure. Carbon yield was determined using [12] method by measuring the sample weight before and after carbonization and calculating the yield. The specific surface area was estimated using the Sear method [13]. Bulk density was measured following [14] by filling a 10 cm^3 centrifuge tube with a known weight of lump-free activated carbon while tapping to eliminate voids. The final weight was recorded, and bulk density was calculated using Equation

1. These measurements provided key physical characteristics essential for evaluating the adsorbents' effectiveness.

$$\text{Bulk Density} = \frac{\textit{Weight of carbon (g)}}{\textit{Volume of dry sample (cm3)}} \quad (1)$$

Collection of PAHs contaminated water: The groundwater study was carried out at Site X in Rumuekpe, Emuoha Local Government Area, Rivers State, Nigeria, positioned at longitude 6°41'25"E and latitude 5°01'41"N. The region is home to multiple oil processing facilities and an extensive crude oil pipeline network. Due to pipeline vandalism, ruptures, and illegal activities, frequent oil spills have been reported. Groundwater samples were collected and analyzed from five wells, each drilled to a depth of 8 meters.

Batch Adsorption studies

Effect of Adsorbent Dosage: Specified adsorbent doses of 0.2, 0.4, 0.6, 0.8, and 1.0 g were added to 50 mL water samples with an initial PAH concentration of 50 mg/L at pH 6. The mixtures were agitated at 150 rpm using a mechanical shaker for optimal contact times of 90 minutes (PSAAC), 60 minutes (CSAAC and CWSAAC), and 120 minutes (WSAAC). Equilibrium studies were conducted at room temperature (25°C). After agitation, the mixtures were filtered using Whatman No. 542 filter paper, and the residual PAH concentrations in the filtrates were analyzed using GC- MS. The equilibrium adsorption capacity (qe) was calculated using Equation (2).

$$q_e = \frac{(C_o - C_e)V}{M}$$

(2)Where: qe = quantity adsorbed (mg/g)Co and Ce = initial and equilibrium concentrations (mg/l) V = Volume (L)
M = mass of adsorbent (g)

Effect of Contact time: The relationship between contact time and the adsorption capacity of the activated carbon samples was investigated. In this experiment, 1 g of each activated carbon sample was added to 50 mL of a PAH standard solution with an initial concentration of 50 mg/L in a conical flask. The samples were collected at 10-minute intervals from 10 to 120 minutes at room temperature. Residual PAH concentrations in the solution were then extracted and analyzed.

PAHs Extraction Method: The liquid-liquid extraction technique described by [15] was employed to extract PAHs from the sampled solutions. PAHs were extracted from the sampled solutions using analytical-grade dichloromethane (DCM) (99.0% purity, Loba Chemie) as the solvent. A 25 mL volume of DCM was added to the solution and vigorously shaken for approximately 2 minutes to promote phase separation, with intermittent venting to release pressure. The extraction process was repeated twice to enhance PAH recovery. The mixture was then left to evaporate at room temperature for six hours. To remove residual moisture, 1 g of anhydrous sodium sulfate was added before transferring 1 mL of the extract into a vial for analysis using an Agilent 7890N GC/MS gas chromatograph.

***Statistical Analysis*:** Studies of T Test were carried out to perform a comparative analysis of the removal efficiencies of the selected adsorbents

Equilibrium Modeling: The adsorption performance of the activated carbons was assessed using various isotherm models, including Henry, Langmuir, Freundlich, Elovich, and Jovanovic models. The XLSTAT 2014 software was utilized to estimate model coefficients via nonlinear optimization. The Henry isotherm was modelled as a single-parameter system, while the Langmuir, Freundlich, Elovich, and Jovanovic models were

treated as two-parameter isotherms. Parameter estimation was performed using an iterative direct optimization method to minimize errors.

3. Results and Discussion

Results of the Adsorbent Characterization Experiments: *The FTIR, and Physicochemical Analysis of the Activated Carbon Prepared:* FT-IR analysis was conducted to identify functional groups on the activated carbon surfaces, with spectra data summarized in Tables 1 and 2. Acid-activated samples exhibited O-H, C-H, C=O, and C-O absorption bands, indicating hydroxyl, aliphatic, ester, and carboxyl groups. The spectra of CSAAC showed prominent bands at 3540, 3394, 1797, and 1616 cm^{-1}, attributed to O-H, C-H, esters C=O, and amides C=O, with similar trends observed in PSAAC, WSAAC, and CWSAAC, suggesting comparable surface functionality. Additional bands at 1150, 1398, 873, and 713 cm^{-1}, assigned to C-O, C-O-C, M-O, and aromatic C-H bending,also appeared across all acid-treated samples, as confirmed in Figure 1, aligning with previous studies [16];[17];[18].

Base-activated samples exhibited similar functional groups but with reduced O-H, C-H, and C-O intensities and the absence of amide C=O bands, attributed to potassium hydroxide treatment [19]. These variations suggest that acid activation introduces more oxygen-containing functional groups, which can enhance hydrophilicity and favor the adsorption of polar contaminants. In contrast, base activation alters the surface chemistry, potentially improving selectivity for non- polar pollutants. Furthermore, the disappearance of amide C=O in base-activated samples suggests the breakdown or removal of nitrogen-containing functional groups due to the strong alkaline conditions. Despite these differences, Figure 2 highlights the overall surface chemical similarities among base-treated samples. These observations confirm that the activation method significantly influences surface chemistry, which in turn affects adsorption efficiency and selectivity.

Table 1: FT-IR spectra data of the acid-activated carbon from crustacean shells

Sample/ band (cm^{-1})	O-H	C-H	C=O	C-O	C-O-C	M-O	Ar-H
CSAAC	3540	3394	1797; 1616	1122	1398	873	713
PSAAC	3540	3394	1789; 1624	1135	1389	864	704
WSAAC	3553	3398	1797; 1620	1135	1393	869	713
CWSAAC	3550	3398	1793; 1616	1126	1397	869	713

Table 2: FT-IR spectra data of the base-activated carbon from crustacean shells

Sample/ band (cm^{-1})	O-H	C-H	C=O	C-O	C-O-C	M-O	Ar-H	
CSBAC	3553	3345	1797	1122	1398	873	713	
PSBAC	3518	3358	1789	1135	1389	864	704	
WSBAC	3576	3389	1793	1135	1393	869	713	
CWSBAC	3523	3336	1789	1126	1397	869	713	

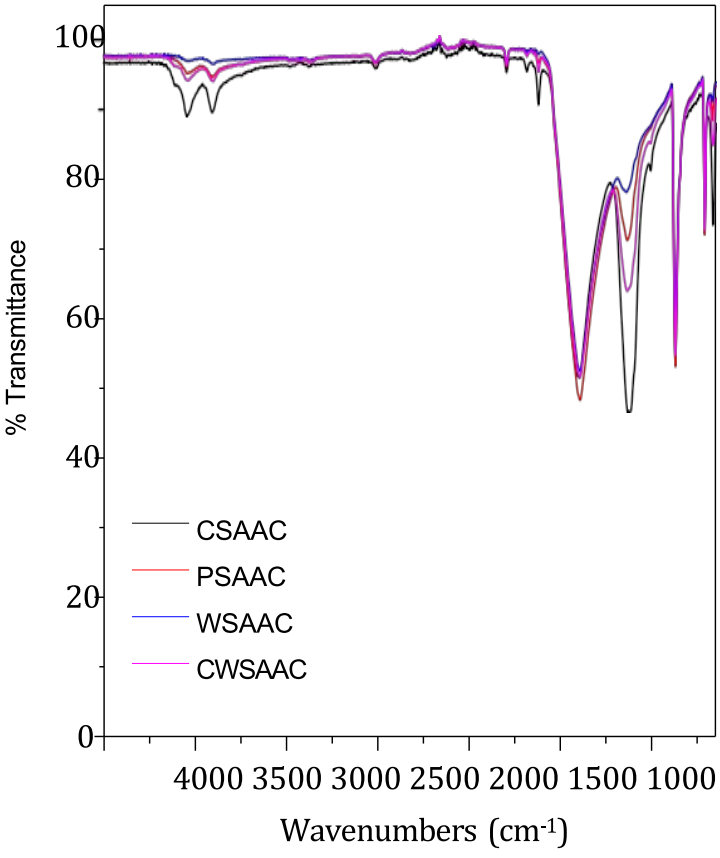

Figure 1: Stacked FT-IR spectra of acid-treated activated carbon

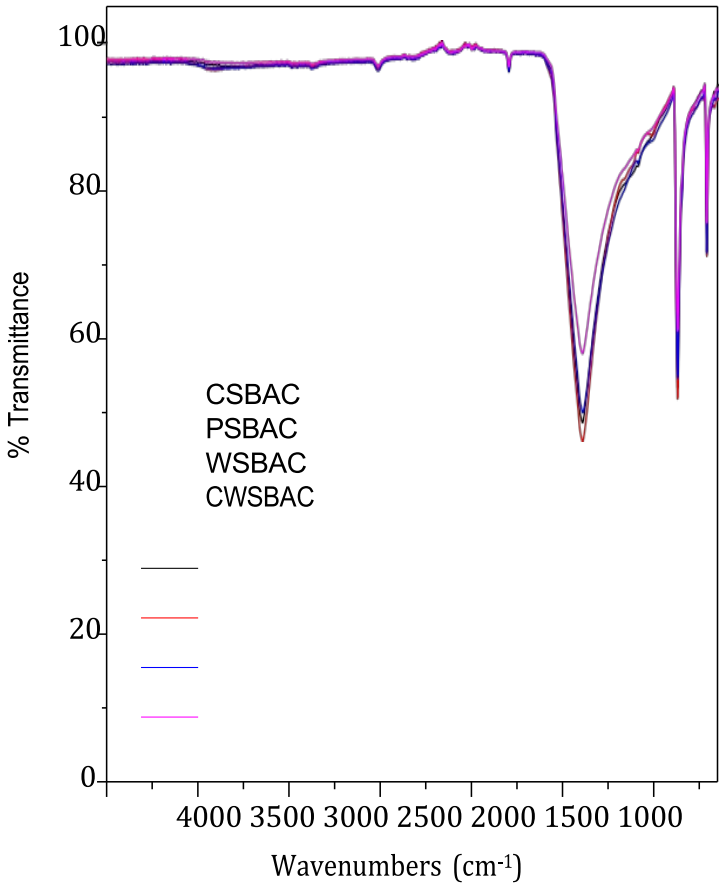

Figure 2: Stacked FT-IR spectra of base-treated activated carbons

Table 3 presents the carbon yield percentages of the activated samples, with acid-activated samples exhibiting higher yields than base-activated ones. The highest yield was observed in CSAAC (87%), while WSBAC had the lowest (71.6%). This aligns with the findings of [20], who reported a 95% yield from activated crustacean shells. A higher carbon yield indicates efficient raw material conversion, which enhances adsorption performance [20]. Bulk density, defined as the mass of activated carbon per unit volume, influences adsorption efficiency, with typical powder. Activated carbon (PAC) has slightly lower values than granular forms. [21] suggested that a bulk density of approximately 0.5 g/cm^3 is suitable for adsorption, and the crustacean shell-based carbons in this study ranged from 0.454 to 0.687 g/cm^3, consistent with [22]. Higher bulk density enables greater adsorbate retention per unit weight, which is beneficial for PAH adsorption. The activated carbon samples exhibited surface areas between 960 and 1288 m^2/g, making them suitable for adsorption applications [23]. Generally, base-activated samples showed slightly higher surface areas than acid-activated ones, with CSBAC and CSAAC recording 1288 and 1277 m^2/g, respectively. Larger surface areas enhance adsorption by increasing active sites for adsorbate interaction, and both carbonization and chemical activation improve adsorption capacity by modifying surface properties [24]. Surface area variations in activated carbon depend on factors such as precursor material, activation method, and production conditions [23].

Table 3: Characterization of Activated Carbon Samples

Parameter/Sample	PSAAC	CSAAC	WSAAC	CWSAAC	PSBAC	CSBAC	WSBAC	CWSBAC
% Carbon Yield	86.2	87	72.1	86.8	84.2	85.2	71.6	86.3
Specific Surface Area	1193	1277	960	1256	1275	1288	986	1270
(m^2/g) Bulk Density (g/cm^3)	0.502	0.653	0.454	0.530	0.524	0.687	0.476	0.543

Results of Batch Adsorption studies

Effect of Adsorbent Dosage on Adsorption Efficiency: Figures 3 and 5 illustrate the effect of adsorbent mass on PAH removal for acid- and base-activated carbons, respectively. As the adsorbent mass increased from 0.2 g to 1 g, the percentage removal also increased for all samples, with CSAAC and CWSAAC achieving up to 98.93% removal, and CSBAC and CWSBAC reaching 98.94%. The initial steep slope (0.2–0.4 g) suggests that adding adsorbent significantly improves removal efficiency due to increased adsorption sites [25]. Beyond 0.4 g, the slope flattens, indicating site saturation and reduced removal efficiency gains [26]. WSAAC and WSBAC consistently exhibited lower adsorption efficiencies, requiring higher masses to achieve similar removal levels as the other adsorbents. Adsorption capacity, as shown in Figures 4.25 and 4.27, followed an inverse trend, decreasing with increasing adsorbent mass due to the dilution effect [27]. CSAAC, CWSAAC, and PSAAC exhibited the highest adsorption capacities at 0.2 g (~10 mg/g), while WSAAC had the lowest (~9.85 mg/g). Similarly, CSBAC, CWSBAC, and PSBAC showed comparable adsorption trends, while WSBAC had the least efficiency. At 1 g, adsorption capacities dropped to ~2.5 mg/g for acid-activated samples and ~3 mg/g for base- activated samples, confirming that increased mass leads to lower adsorption efficiency per gram of adsorbent [28]. The findings highlight the balance between higher removal efficiency and reduced adsorption capacity, emphasizing the need to optimize adsorbent dosage for efficient and cost-effective PAH removal. These results are consistent with previous studies on adsorption performance [29];[30].

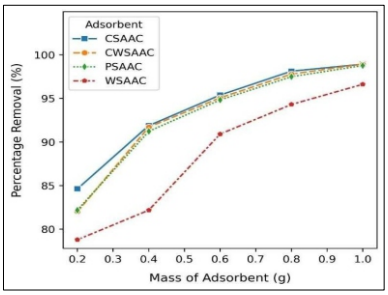

Figure 3: Effect of adsorbent mass on percentage removal for acid-activated carbon

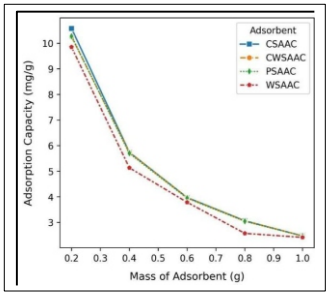

Figure 4: Effect of adsorbent mass on adsorption capacity for acid-activated carbon

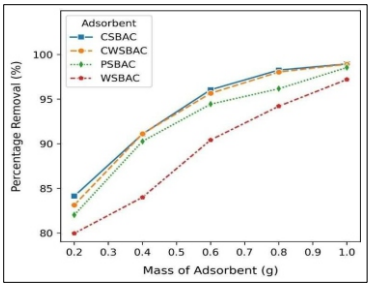

Figure 5: Effect of adsorbent mass on percentage removal for base-activated carbon

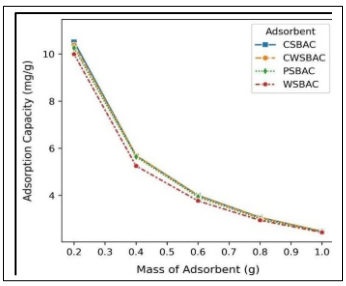

Figure 6: Effect of adsorbent mass on adsorption capacity for base-activated carbon

Effect of Contact time on adsorption capacity: The adsorption experiment in Figure 7 showed that at 10 minutes, PSAAC, CSAAC, and CWSAAC exhibited higher adsorption capacities than WSAAC, with values of 2.269 mg/g, 2.296 mg/g, and 2.358 mg/g, respectively, while WSAAC had 1.994 mg/g. This suggests that WSAAC adsorbed less PAH per gram of adsorbent, while CSAAC performed the best initially. Adsorption capacities increased over time, with CSAAC, CWSAAC, and PSAAC reaching equilibrium at 60–90 minutes, while WSAAC continued. Increasing steadily, reaching 2.37 mg/g after 100 minutes. The highest adsorption capacity was observed for CWSAAC (2.473 mg/g), followed by PSAAC (2.469 mg/g) and CSAAC (2.3 mg/g). The ANOVA results in Table 4 confirmed significant differences among the four acid-activated carbons (F(3,31) = 11.667, p < 0.0001). Tukey's test results in Table 5 grouped CSAAC, PSAAC, and CWSAAC, indicating no significant differences in their adsorption capacities, while WSAAC was in a separate group due to significantly lower performance. This suggests that WSAAC's activation process or intrinsic properties are less effective.

Similarly, the adsorption experiment in Figure 8 showed that at 10 minutes, CSBAC, CWSBAC, and PSBAC exhibited higher adsorption capacities than WSBAC, with values of 2.315 mg/g, 2.295 mg/g, and 2.256 mg/g, respectively, while WSBAC had 1.96 mg/g. Adsorption capacities increased with time, with CSBAC, CWSBAC, and PSBAC reaching equilibrium around 60–90 minutes, whereas WSBAC continued increasing to 2.362 mg/g at 100 minutes. The highest adsorption capacity was observed for CSBAC (2.49 mg/g), followed by CWSBAC (2.473 mg/g) and PSBAC (2.263 mg/g). The ANOVA results in Table 6 confirmed significant differences among the four base-activated carbons (F(3,31) = 9.408, p < 0.0001).

Tukey's test results in Table 7 placed CSBAC, CWSBAC, and PSBAC in the same group, while WSBAC was separate due to lower adsorption performance. These findings highlight the importance of activation methods in determining adsorption efficiency, with CSBAC, CWSBAC, and PSBAC performing better than WSBAC.

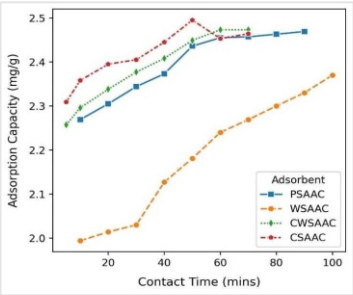

Figure 7: Adsorption Capacity of acid-activated carbon against the contact time

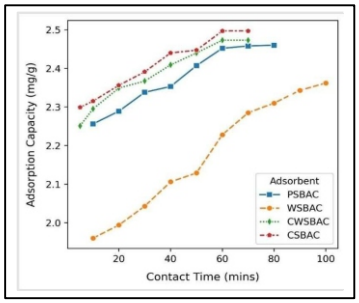

Figure 8: Adsorption Capacity of base-activated carbon against the contact time

Table 4: Analysis of Variance of the Adsorption Capacity based on Contact Time for the different Acid activated carbon

Source	DF	Sum of squares	Mean squares	F	Pr > F
Model	3	0.329	0.110	11.677	< 0.0001
Error	31	0.291	0.009		
Corrected Total	34	0.619			

Computed against model Y=Mean(Y)

Table 5: Tukey Test

Category	LS means	Standard error	Lower bound (95%)	Upper bound (95%)	Groups
CSAAC	2.416	0.034	2.346	2.485	A
PSAAC	2.397	0.032	2.331	2.463	A
CWSAAC	2.384	0.034	2.314	2.454	A
WSAAC	2.186	0.031	2.123	2.248	B

Table 6: Analysis of Variance of the Adsorption Capacity based on Contact Time for the different Base activated carbon

Source	DF	Sum of squares	Mean squares	F	Pr > F
Model	3	0.313	0.104	9.408	0.000
Error	31	0.344	0.011		
Corrected Total	34	0.657			

Computed against model Y=Mean(Y)

Table 7: Tukey Test

Category	LS means	Standard error	Lower bound (95%)	Upper bound (95%)	Groups
CSBAC	2.405	0.037	2.329	2.481	A
CWSBAC	2.382	0.037	2.306	2.458	A
PSBAC	2.364	0.035	2.292	2.436	A
WSBAC	2.176	0.033	2.108	2.244	B

Comparative Analysis: Figure 9 illustrates that CSAAC and CSBAC exhibited increasing adsorption capacities with increasing equilibrium concentrations, with CSBAC performing better at lower concentrations and CSAAC excelling at higher concentrations. Similarly, Figure 10 illustrates that PSAAC consistently outperformed PSBAC across all equilibrium concentrations, with both.Adsorbents reaching approximately 10 mg/g at 8 mg/L, demonstrating strong PAH removal efficiency. Figure 11 shows that WSAAC and WSBAC followed similar adsorption trends, although WSBAC exhibits a slightly higher adsorption capacity at higher equilibrium concentrations (6 mg/g at 9 mg/L vs. 5 mg/g for WSAAC). In Figure 12, CWSAAC marginally outperformed CWSBAC at higher equilibrium concentrations, achieving 9 mg/g at 7 mg/L, while CWSBAC reaches 8.6 mg/g. T-test results in Tables 8 to 11 indicate no significant difference in adsorption capacities between acid- and base-activated carbons, confirming their comparable effectiveness. A comparative analysis of the effect of time was carried out. Figure 13 displays adsorption over time for CSAAC and CSBAC, showing rapid uptake in the first 50–60 minutes, after which CSAAC declines while CSBAC stabilizes. This trend is noted in the comparative analysis in Figures 14 and 15, which depict adsorption trends over time for WSAAC and WSBAC; CWSAAC and CWSBAC, respectively, with adsorption peaking at 60–100 minutes before stabilizing or declining. T-test results in Tables 12 to 14 indicate no statistically significant differences in adsorption performance between acid- and base-activated carbons, suggesting similar efficiency. Across all cases, the rapid initial adsorption is attributed to active site availability, followed by equilibrium or decline due to site saturation, confirming that both activation methods yield effective adsorbents for PAH removal with minimal differences in performance [31];[32].

Table 8: T-test to check for significance in clamshell adsorbent capacity between the acid and base activated carbon

Difference 0.015
t (Observed value) 0.007
|t| (Critical value) 2.306
DF 8
p-value (Two-tailed) 0.994
alpha 0.05

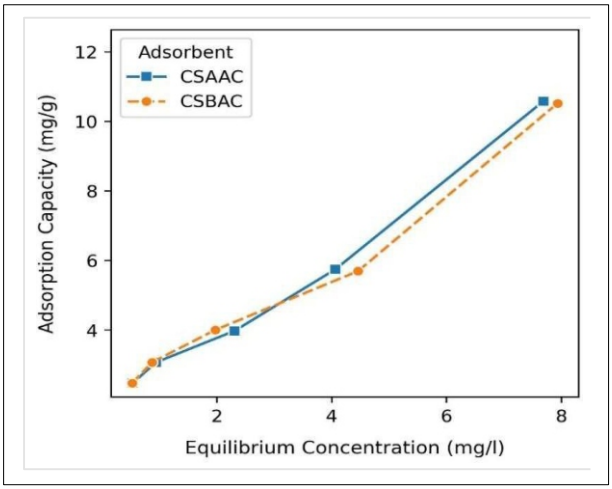

Fig 9: Comparative Analysis of the Acid and base activated Clam Shell

Table 9: T-test to check for significance in the adsorbent capacity between the acid and base-activated carbon for periwinkle shell

Difference 0.029
t (Observed value) 0.014
|t| (Critical value) 2.306
DF 8
p-value (Two-tailed) 0.989
alpha 0.05

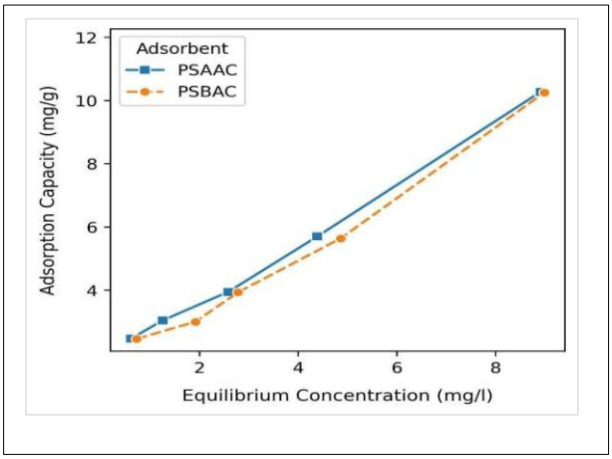

Fig 10: Comparative Analysis of the Acid and base-activated Periwinkle Shell

Table 10: T-test to check for significance in the adsorbent capacity between the acid and base activated carbon for whelk shell

Difference -0.126
t (Observed value) -0.065
|t| (Critical value) 2.306
DF 8
p-value (Two-tailed) 0.950
alpha 0.05

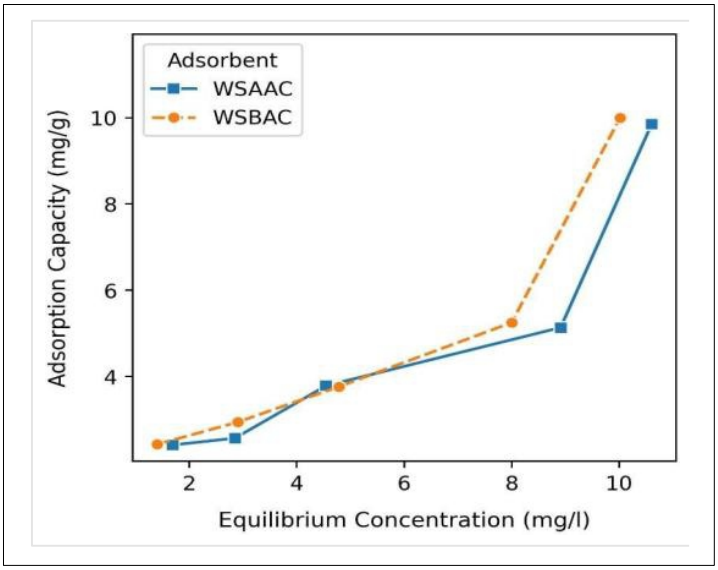

Fig 11: Comparative Analysis between the Acid and base-activated Whelk Shell

Table 11: T-test to check for significance in the adsorbent capacity between the acid and base activated carbon for Clam-Whelk shell

Difference -0.027
t (Observed value) -0.014
|t| (Critical value) 2.306
DF 8
p-value (Two-tailed) 0.989
alpha 0.05

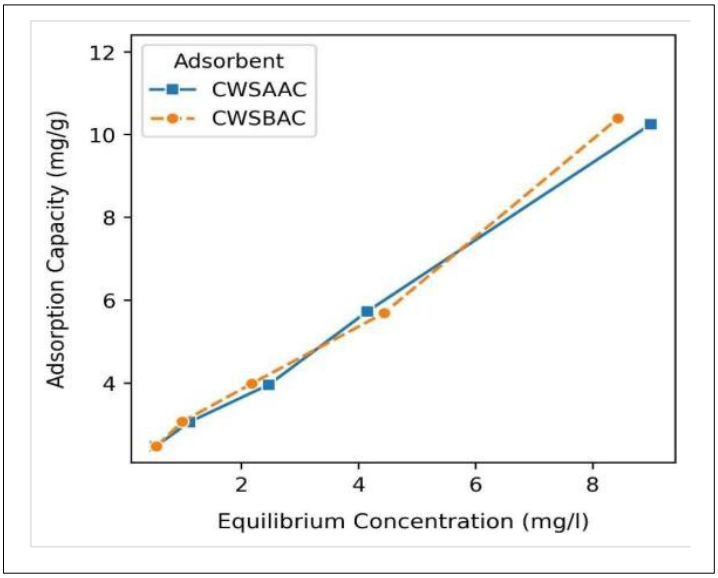

Fig 12: Comparative Analysis between the Acid and base activated Clam-Whelk Shell

Table 12: T-test to check for significance in the adsorbent capacity between the acid and base activated carbon for Clam shell (As a function of time)

Difference 0.010
t (Observed value) 0.294
|t| (Critical value) 2.145
DF 14
p-value (Two-tailed) 0.773
alpha 0.05

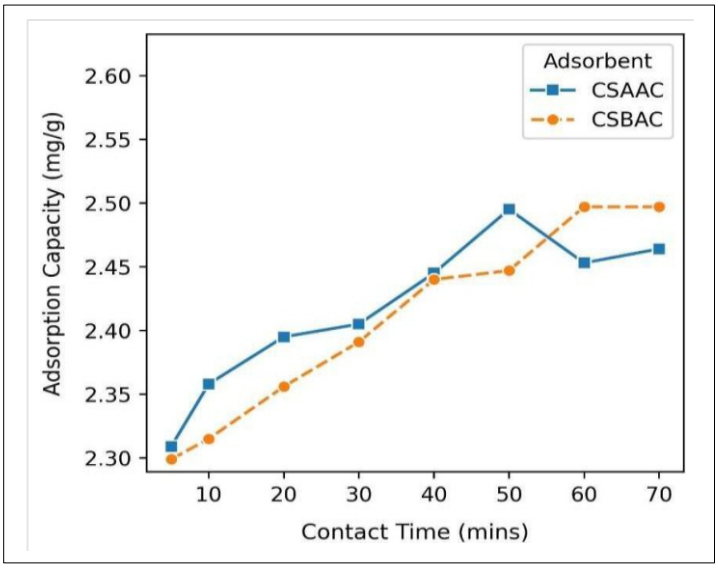

Fig 13: Comparative Analysis between the Acid and base activated Clam Shell (As a function of Time)

Table 13: T-test to check for significance in the adsorbent capacity between the acid and base activated carbon for Whelk shell (As a function of time)

Difference 0.010
t (Observed value) 0.148
|t| (Critical value) 2.101
DF 18
p-value (Two-tailed) 0.884
alpha 0.05

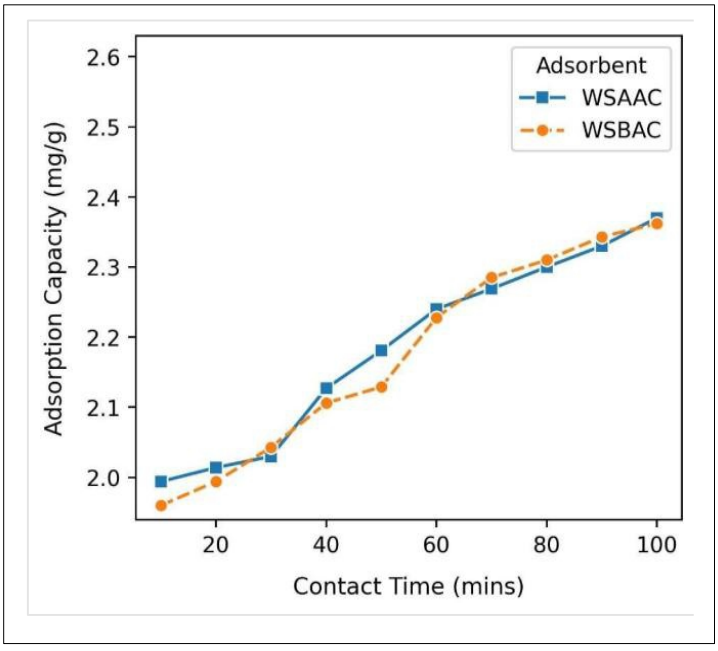

Fig 14: Comparative Analysis between the Acid and base activated Whelk Shell (As a function of Time)

Table 14: T-test to check for significance in the adsorbent capacity between the acid and base activated carbon for the Clam-Whelk shell (As a function of time)

Difference 0.002
t (Observed value) 0.043
|t| (Critical value) 2.145
DF 14
p-value (Two-tailed) 0.966
alpha 0.05

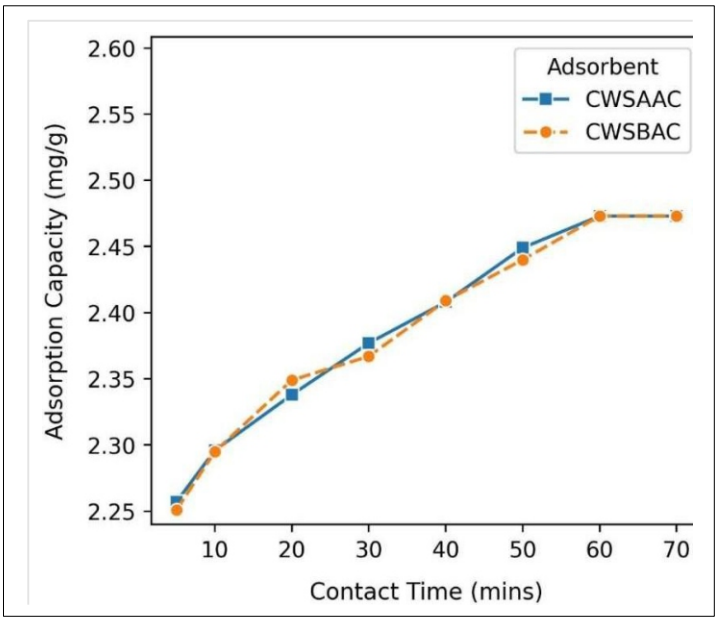

Fig 15: Comparative Analysis between the Acid and base activated Clam-Whelk Shell (As a function of Time)

Adsorption Isotherm Models: The result from the isotherm models for Henry, Langmuir, Freundlich, Elovich and Janovich constants for PAH adsorption in Table 15 indicated that the equilibrium data fitted the Freundlich isotherm better for PSAAC, CSAAC, CWSAAC, PSBAC, CSBAC and CWSBAC with the highest coefficient of determination while Henry Isotherm was a better fit for WSAAC and WSBAC. The resultant Freundlich exponent values n for PSAAC, CSAAC, CWSAAC, PSBAC, CSBAC and CWSBAC were noted as 1.528,1.503, 1.632, 1.329,1.633 and 1.621, respectively. This signifies a high adsorption rate as the ideal values for the exponent n lying between 0 and 10 suggest favorable adsorption [33];[34];[35]. This implies that the activated samples are heterogeneous with sites of varying affinities and have a varied surface with multiple adsorption sites, each with different adsorption energies, which is better captured by the Freundlich model than by other models [36]. The Freundlich constant KL indicates the adsorption capacity, and it is noted that CSBAC presented the maximum adsorption capacity for the isotherm at a value of 2.770mg/g. The Henry isotherm model best described the adsorption behaviour of WSAAC and WSBAC with R^2 values of 0.816 and 0.835 and a Henry constant (KHE) of 0.800 and 0.871, respectively. This suggests that the adsorption process for WSAAC and WSBAC follows a linear isotherm, indicative of low-concentration adsorption states or infinite dilution, where the adsorbate molecules do not interact with each other, and the surface sites are uniformly available [37];[38];[39]. The results also indicated that the Coefficient of determination (R^2) for Freundlich isotherm for PSAAC, CSAAC, CWSAAC, PSBAC, CSBAC and CWSBAC was 0.970, 0.952,0.971,0.966,0.940 and 0.956; Langmuir Isotherm was 0.941,0.923,0.937,0.9510.898 and 0.917 while Janovich was 0.939,0922, 0.934,0.951,0.897 and 0.915 respectively. The results indicate that the adsorption patterns for PAHs followed the Langmuir and Freundlich isotherms (as Janovich isotherm is established on the assumptionscontained in the Langmuir model). According to [40] and [41], any adsorption system which obeys both the Freundlich and Langmuir isotherms shows that the solute forms a homogenous monolayer on the adsorbate. This implies that the adsorption of PAHs onto PSAAC, CSAAC, CWSAAC, PSBAC, CSBAC and CWSBAC obeyed both Freundlich and Langmuir isotherms, signifying that the PAHs formed a monolayer on the surfaces of the adsorbents. The maximum adsorption capacity for monolayer Qm from Table 4.33 was compared between Langmuir and Janovich isotherms and it was noted that Langmuir Isotherm presented the highest adsorption capacities for PSAAC, CSAAC, CWSAAC, PSBAC, CSBAC and CWSBAC with values of 21.247, 23.995, 18.719, 31.688, 18.335 and 18.743 mg/g respectively while Janovich Isotherm presented a higher maximum capacity for WSAAC and WSBAC at 10.970 and 10.362 mg/g respectively.

Table 15: Isotherm Modeling for Activated Samples

Number of Isotherm Type Model Carbon Activator Types

parameters	Model	Parameters	PSAAC	CSAAC	WSAAC	CWSAAC	PSBAC	CSBAC	WSBAC	CWSBAC
One- Parameter	Henry	KHE	1.232	1.438	0.800	1.234	1.187	1.376	0.871	1.301
	Langmuir	R^2	0.908	0.909	0.816	0.890	0.939	0.886	0.835	0.892
		Qm	21.247	23.995	8.864	18.719	31.688	18.335	9.133	18.743
		b	0.099	0.095	2.144	0.126	0.051	0.144	2.131	0.131
		R^2	0.941	0.923	0.812	0.937	0.951	0.898	0.834	0.917
Two- Parameters	Freundlich	Kf	2.374	2.590	0.970	2.587	1.901	2.770	0.908	2.649
		n	1.528	1.503	1.099	1.632	1.329	1.633	1.020	1.621
	Elovich	R^2	0.970	0.952	0.797	0.971	0.966	0.940	0.831	0.956
		β	0.364	0.366	0.299	0.385	0.339	0.380	0.317	0.380
		α	7.324	8.818	3.008	8.300	5.867	9.306	3.406	8.664
	Jovanovic	R^2	0.797	0.767	0.591	0.805	0.742	0.787	0.512	0.799
		Qm	14.214	16.059	10.970	12.976	19.316	13.416	10.362	13.322
		Kf	0.137	0.132	0.005	0.164	0.082	0.170	0.000	0.163
		R^2	0.939	0.922	0.812	0.934	0.951	0.897	0.834	0.915

Qm = Maximum monolayer adsorption capacity (mg/g), KHE = Henry's adsorption constant, b = Langmuir constant (L/mg), R^2 = Coefficient of determinants, KF = Affinity factor (mg/g)(L/mg)$^{1/n}$, n = Freundlich exponent, α =initial rate constant (mg/g * min), β=desorption constant (mg/g)*

***Adsorption Summary**:* The levels of Polycyclic Aromatic Hydrocarbons (PAHs) in contaminated groundwater before and after treatment with different activated carbon samples are shown in Table 16. The results demonstrated the robust adsorptive performance of the produced carbons by yielding a significant drop in PAH concentrations after adsorption, with many components reduced to non-detectable levels (N.D.). The samples of activated carbon successfully eliminated a variety of PAH components, indicating their potential for thorough groundwater purification. The adsorption process's effectiveness was further supported by the fact that measurable PAH residual concentrations were much lower than starting levels. These results highlighted how well-suited the produced activated carbon composites are for the removal of PAHs from contaminated water sources.

Table 16: PAHs contamination before and after Adsorption with activated carbon samples

S/N	PAHs Individual Components	Water sample Value before adsorption (mg/l)	Water sample Value after adsorption (mg/l) PSAAC	Water sample Value after adsorption (mg/l) CSAAC	Water sample Value after adsorption (mg/l) WSAAC	Water sample Value after adsorption (mg/l) CWSAAC	Water sample Value after adsorption (mg/l) PSBAC	Water sample Value after adsorption (mg/l) CSBAC	Water sample Value after adsorption (mg/l) WSBAC	Water sample Value after adsorption (mg/l) CWSBAC
	1. Naphthalene	1.680	N.D	N.D	N.D	N.D	N.D	N.D	N.D	N.D
	2. Acenaphthylene	2.997	N.D	0.04936	0.1960	0.04887	0.04884	0.04924	0.0406	N.D
	3. Acenaphthene	2.404	0.05878	N.D	0.0368	N.D	0.05170	0.05711	0.0789	0.04998
	4. Fluorene	2.134	0.04978	0.04906	0.2724	0.04902	0.04965	0.04958	0.0147	0.04952
	5. Phenanthrene	0.630	0.05153	0.04996	0.1175	0.04918	0.08918	0.05156	0.2653	0.04993
	6. Anthracene	1.041	0.05017	0.04844	0.0602	0.04759	0.09131	0.05020	0.1138	0.04841
	7. Fluoranthene	1.135	0.05087	0.04915	0.0324	0.04950	0.05037	0.04941	0.0147	0.05064
	8. Pyrene	2.871	0.04962	0.04964	0.2017	0.04918	0.04962	0.05048	0.0794	0.05133
	9. Benz(a)anthracene	2.808	0.03484	N.D	0.0329	0.00009	0.00550	N.D	0.0018	N.D
	10. Chrysene	3.376	N.D	N.D	0.0676	N.D	0.05248	0.02506	0.0206	N.D
	11. Benzo(b)fluoranth ene	3.310	0.03	N.D	0.0072	N.D	N.D	N.D	0.0175	N.D
	12. Benzo(k)fluoranth ene	5.861	0.04832	0.04805	0.1319	0.04805	0.04822	N.D	0.0173	0.04894
	13. Benzo(a)pyrene	4.331	0.04815	0.04786	0.1865	0.04783	0.04802	N.D	0.1738	0.04883
	14. Benzo(ghi) perylene	4.933	0.04862	0.04850	0.2101	0.04839	0.04856	0.04855	0.3028	0.04889
	15. Dibenz(a,h) anthracene	2.571	0.04870	0.04863	0.0123	0.04863	0.04865	0.04860	0.1544	0.04909
	16. Indeno(1,2,3) perylene	7.913	0.04978	0.04967	0.1265	0.04925	0.04937	0.04970	0.1064	0.04969
	∑16 PAHs	**50.003**	**0.616**	**0.538**	**1.692**	**0.536**	**0.731**	**0.529**	**1.402**	**0.545**
	DPR Limit	**70**	**70**	**70**	**70**	**70**	**70**	**70**	**70**	**70**

N.D = Not Detectable

4. Conclusion

This study demonstrated the potential of marine shell wastes—periwinkle, clam, whelk, and clam-whelk composites—as effective raw materials for producing activated carbon for PAH removal from contaminated water. High removal efficiencies were produced by both base and acid activation techniques. Also, CSBAC proved to be the most successful in the removal of PAHs with an efficiency of 98.94%. The characterization results showed notable differences in functional groups and surface area, affecting adsorption effectiveness. Most samples' adsorption data suited the Freundlich and Langmuir isotherms well, but the Henry model provided a more accurate description of the carbons obtained from whelk. Significantly, statistical analysis showed no discernible difference between base and acid activation techniques, indicating that either approach is feasible based on application objectives and resource availability. These findings highlighted the value of sustainable waste valorization for environmental remediation and offer a promising approach for low-cost, efficient treatment of PAH-contaminated water systems.

Disclaimer (Artificial Intelligence)

Author(s) hereby declare that NO generative AI technologies such as Large Language Models (Chatgpt, COPILOT, etc) and text-to-image generators were used during the writing or editing of this manuscript.

Competing Interests

The authors have declared that no competing interests exist.

References

1. Crini G, Lichtfouse E, Wilson L. D & Crini N.M (2018) Adsorption-Oriented Processes Using Conventional & Non-conventional Adsorbents for Wastewater Treatment. https://doi.org/10.1007/978-3-319-92111-2_2

2. Azizian S & Eris S. (2020). Adsorption isotherms and kinetics. *Interface Science & Technology*, *33*, 445-509. https://doi.org/10.1016/B978-0-12-818805-7.00011-4

3. Khulbe K. C & Matsuura T (2018) Removal of heavy metals & pollutants by membrane adsorption techniques. https://doi.org/10.1007/s13201-018-0661-6

4. Akomah U, Nwaogazie I. L & Akaranta O (2021) A Review on Current Trends in Heavy Metal Removal from Water between 2000-2021. *International Journal of Environment and Climate Change* 11(12): 67-90. https://doi.org/10.9734/ijecc/2021/v11i1230557

5. Othmani, A., John, J., Rajendran, H., Mansouri, A., Sillanpää, M. & Velayudhaperumal C.P. (2021). Biochar & activated carbon derivatives of lignocellulosic fibers towards adsorptive removal of pollutants from aqueous systems: Critical study & future insight. *Separation & Purification Technology*, *274*, 119062. https://doi.org/10.1016/j.seppur.2021.119062

6. Ani, J.U., Akpomie, K.G., Okoro, U.C., Aneke L.E, Onukwuli O.D & Ujam O.T (2020). Potentials of activated carbon produced from biomass materials for sequestration of dyes, heavy metals, and crude oil components from aqueous environment. *Appl Water Sci* 10, 69 . https://doi.org/10.1007/s13201-020-1149-8

7. González-García, P. (2018). Activated carbon from lignocellulosics precursors: A review of the synthesis methods, characterization techniques & applications. *Renewable & Sustainable Energy Reviews*, *82*, 1393-1414. https://doi.org/10.1016/j.rser.2017.04.117

8. Salleh, M. A. M., Mahmoud, D. K., Karim, W. A. W. A., & Idris, A. (2011). Cationic & anionic dye adsorption by agricultural solid wastes: A comprehensive review. *Desalination*, *280*(1-3), 1-13. https://doi.org/10.1016/j.desal.2011.07.019

9. Foong, S. Y., Liew, R. K., Yek, P. N., Chan, Y. H. & Lam, S. S. (2024). A Review in Production of Nitrogen-Enriched Carbon Materials via Chitin Pyrolysis & Activation for Enhanced Wastewater Remediation. *Current Opinion in Green and Sustainable Chemistry*, 100920. https://doi.org/10.1016/j.cogsc.2024.100920

10. Kumari, R., Kumar, M., Vivekanand, V., & Pareek, N. (2023). Chitin biorefinery: A narrative & prophecy of crustacean shell waste sustainable transformation into bioactives & renewable energy. *Renewable & Sustainable Energy Reviews*, *184*, 113595. https://doi.org/10.1016/j.rser.2023.113595

11. Magnacca, G., Guerretta, F., Vizintin, A., Benzi, P., Valsania, M. C. & Nisticò, R. (2017). Preparation, characterization and environmental/electrochemical energy storage testing of low-cost biochar from natural chitin obtained via pyrolysis at mild conditions. *Applied Surface Science*, *427*, 883-893. https://doi.org/10.1016/j.apsusc.2017.07.277

12. Fapetu, O. P. (2000). Production of charcoal from tropical biomass for industrial and metallurgical process. *Nigerian Journal of Engineering Management*, 1(2), 34- 37.

13. Abate G. Y , Adugna N.A, Adere T. H & Desiew M.G (2020) Adsorptive removal of malachite green dye from aqueous solution onto activated carbon of Catha edulis stem as a low cost bio-adsorbent. https://doi.org/10.1186/s40068-020-00191-4

14. Efeovbokhan V.E , Alagbe E.E, Odika B, Babalola R,Oladimeji T.E, Abatan O.G. & Yusuf E.O. (2019) Preparation & characterization of activated carbon from plantain peel & coconut shell using biological activators. doi:10.1088/1742- 6596/1378/3/032035

15. Assad A. A, Gaber S. E & Jahin H. S (2019) Removal of Polycyclic Aromatic Hydrocarbons from Water Utilizing Activated Carbons. *World Journal of Chemistry* 14 (1): 22-32. DOI: 10.5829/idosi.wjc.2019.22.32

16. Akpan, E. I., Gbenebor, O. P., & Adeosun, S. O. (2018). Synthesis and characterisation of chitin from periwinkle (Tympanotonus fusatus (L.)) and snail (Lissachatina fulica (Bowdich)) shells. *International journal of biological macromolecules*, 106, 1080-1088.

17. Kunusa, W. R., Iyabu, H., & Abdullah, R. (2021). FTIR, SEM, & XRD analysis of activated carbon from sago wastes using acid modification. *In Journal of Physics: Conference Series* 1968 (1) 012014.

18. Okoya, A. A., & Diisu, D. (2021). Research Article Adsorption of Indigo-dye from Textile Wastewater onto Activated Carbon Prepared from Sawdust & Periwinkle Shell. http://dx.doi.org/10.3923/tasr.2021.1.9

19. Eke-emezie, N., Etuk, B.R., Akpan, O.P & Okechukwu C.C (2022) Cyanide removal from cassava wastewater onto H3PO4 activated periwinkle shell carbon. *Appl Water Sci* 12, 157. https://doi.org/10.1007/s13201-022-01679-3

20. Oyedoh E.A & Ekesiobi U. U. (2023). Effects of Preparation Conditions on Surface Properties & Yields of Periwinkle Shell Activated Carbon. *J. Appl. Sci. Environ. Manage*. 27 (6) 1083-1091. https://dx.doi.org/10.4314/jasem.v27i6.6

21. Okieimen F.E., Okiemen, C.O. & Wuana, R.A. (2007): Preparation & Characterization of Activated Carbon from Rice Husks, *J. of Chem. Soc.,* Vol. 32: 126-136.https://www.researchgate.net/publication/288024125_Preparation_&_charact_erization_of_activated_carbon_from_rice_husks/citations

22. Madojemu, G., Eze, C. B., & Okieimen, F. (2020). OPTIMIZATION OF SURFACE AREA OF ACTIVATED CARBONS PREPARED FROM COCONUT SHELLS BY RESPONSE SURFACE METHODOLOGY. *Journal of Chemical Society of Nigeria*, *45*(2). https://journals.chemsociety.org.ng/index.php/jcsn/article/view/460

23. Ngu, L. H. (2023). Carbon Capture Technologies. *Encyclopedia of Sustainable Technologies (Second Edition)*, 358-377. https://doi.org/10.1016/B978-0-323- 90386-8.00028-0

24. Mopoung S. & Nogklai, W.(2008)Chemical and surface properties of longan seed activated charcoal. https://doi.org/10.5897/IJPS.9000116

25. Hedayati, M. S. & Li, L. Y. (2020). Removal of polycyclic aromatic hydrocarbons from aqueous media using modified clinoptilolite. *Journal of Environmental Management*, *273*, 111113.https://doi.org/10.1016/j.jenvman. 2020.111113

26. Huang, Y., Fulton, A. N. & Keller, A. A. (2016). Simultaneous removal of PAHs and metal contaminants from water using magnetic nanoparticle adsorbents. *Science of The Total Environment*, *571*, 1029-1036. https://doi.org/10.1016/j.scitotenv.2016.07.093

27. Alomar, T.S., Habila, M.A., AlMasoud, N., Alothman, Z.A., Sheikh, M. & Soylak, M. (2021) Biomass-Derived Adsorbent for Dispersive Solid-Phase Extraction of Cr (III), Fe (III), Co (II) and Ni (II) from Food Samples Prior to ICP-MS.Detection. *Appl. Sci.* 2021, 11, 7792. https://doi.org/10.3390/app11177792

28. Patrulea. V, Anamaria N, Manuela M. M, Laura D. P, Otilia B. S, & Vasile O (2013) Optimization of the Removal of Copper (II) Ions from Aqueous Solution on Chitosan & Cross-Linked Chitosan Beads. DOI: 10.15376/biores.8.1.1147-1165

29. Wang Z., Zheng X., Wang, Y., Lin, H., & Zhang, H. (2022). Evaluation of phenanthrene removal from soil washing effluent by activated carbon adsorption using response surface methodology. *Chinese Journal of Chemical Engineering*, *42*, 399-405. https://doi.org/10.1016/j.cjche.2021.02.027

30. Pathak, S., Sakhiya, A. K., An&, A., Pant, K., & Kaushal, P. (2022). A state-of- the-art review of various adsorption media employed for the removal of toxic Polycyclic aromatic hydrocarbons (PAHs): An approach towards a cleaner environment. *Journal of Water Process Engineering*, *47*, 102674. https://doi.org/10.1016/j.jwpe.2022.102674

31. Issabayeva, G., Wong, S.H., Pang, C.Y, Wong M.C & Aroua M.K (2022). Fluoride removal by low-cost palm shell activated carbon modified with prawn shell chitosan adsorbents. *Int. J. Environ. Sci. Technol.* 19, 3731–3740. https://doi.org/10.1007/s13762-021-03448-2

32. Adeleke, A. O., Omar, R., Katibi, K. K., Dele-Afolabi, T. T., Ahmad, A., Quazim, J. O., Amusa, A. A., & Alshammari, M. B. (2024). Process optimization of superior biosorption capacity of biogenic oyster shells nanoparticles for Congo red & Bromothymol blue dyes removal from aqueous solution: Response surface methodology, equilibrium isotherm, kinetic, and reusability studies. *Alexandria Engineering Journal*, *92*, 11-23. https://doi.org/10.1016/j.aej.2024.02.042

33. Tran, H. N., You, S., Hosseini-Bandegharaei, A. & Chao, H. (2017). Mistakes and inconsistencies regarding adsorption of contaminants from aqueous solutions: A critical review. *Water Research*, *120*, 88-116. https://doi.org/10.1016/j.watres.2017.04.014

34. Rolph C.A, Jefferson B, Hassard F & Villa R (2018) Metaldehyde removal from drinking water by adsorption onto filtration media: mechanisms and optimization. http://dx.doi.org/10.1039/C8EW00056E

35. Kumar, U. & Bandyopadhyay, M. (2005). Sorption of cadmium from aqueous solution using pretreated rice husk. *Bioresource Technology*, *97*(1), 104-109. https://doi.org/10.1016/j.biortech.2005.02.027

36. Kumar, J. A., Amarnath, D. J., Sathish, S., Jabasingh, S. A., Saravanan, A., Hemavathy, R., Anand, K. V., & Yaashikaa, P. (2019). Enhanced PAHs removal using pyrolysis-assisted potassium hydroxide induced palm shell activated carbon: Batch & column investigation. *Journal of Molecular Liquids*, *279*, 77-87. https://doi.org/10.1016/j.molliq.2019.01.121

37. Ayawei N, Augustus N. E, & Donbebe W (2017). Modelling and Interpretation of Adsorption Isotherms. https://doi.org/10.1155/2017/3039817

38. Deocaris C.C & Osio L.P (2020) Fitting Henry's Adsorption Isotherm model in R using PUPAIM package. https://www.researchgate.net/publication/342039215_Fitting_Henry%27s_Adsor_ption_Isotherm_model_in_R_using_PUPAIM_package?enrichId=rgreq-_b9c5374807dae2b2dd2b75647a7fd128-_XXX&enrichSource=Y292ZXJQYWdlOzM0MjAzOTIxNTtBUzo5MDA0MjMwMTk5Mzc3OTJAMTU5MTY4ODk4NTEyMg%3D%3D&el=1_x_2

39. Ehiomogue, P., Ahuchaogu, I. I., & Ahaneku, I. E. (2021). REVIEW OF ADSORPTION ISOTHERMS MODELS. *Acta Technica Corviniensis-Bulletin of Engineering*, *14*(4). https://acta.fih.upt.ro/pdf/archive/ACTA-2021-4.pdf

40. Das, D. D., Mahapatra, R., Pradhan, J., Das, S. N., & Thakur, R. S. (2000). Removal of Cr(VI) from Aqueous Solution Using Activated Cow Dung Carbon. *Journal of Colloid & Interface Science*, *232*(2), 235-240. https://doi.org/10.1006/jcis.2000.7141

41. Sathish, T., Vinithkumar, N.V., Dharani, G.& Kirubagaran R (2015) Efficacy of mangrove leaf powder for bioremediation of chromium (VI) from aqueous solutions: kinetic and thermodynamic evaluation. *Appl Water Sci* 5, 153–160. https://doi.org/10.1007/s13201-014-0174-x